JOURNAL OF GUIDANCE, CONTROL, AND DYNAMICS
Vol. 20, No. 6, November–December 1997

Sequential Loop Closure in Design of a Robust Rotorcraft Flight Control System

Peter J. Gorder*
Kansas State University, Manhattan, Kansas 66506
and
Ronald A. Hess†
University of California, Davis, Davis, California 95616

Rotorcraft flight control systems present many significant design challenges. First, large variations in the response characteristics of rotorcraft result from the wide range of airspeeds of typical operation (hover to over 100 kn). Second, the assumption of vehicle rigidity often employed in the design of fixed-wing flight control systems is rarely justified in rotorcraft where rotor degrees of freedom can have a significant impact on the system performance and stability. A methodology is proposed for the design of robust rotorcraft flight control systems utilizing quantitative feedback theory (QFT). QFT is a technique that accounts for variability in the dynamic response of the controlled element in the design of robust control systems. It was developed to address a multiple-input/single-output (MISO) design problem, but the extension of this technique to address multiple-input/multiple-output (MIMO) systems was employed to address the flight control system (FCS) design of a UH-60 Black Hawk Helicopter. This was accomplished by constructing a set of MISO systems mathematically equivalent to the MIMO system. QFT was applied to each member of the set independently. Inherent conservatism in this design technique leads to limitations in its utility. A second approach utilizing the sequential closure of control loops proved an improved method for designing of robust MIMO FCSs. An analysis of the two FCS design methodologies is presented.

I. Introduction

THE design of rotorcraft flight control systems (FCSs) is complicated by the large variations in the response characteristics of the rotorcraft resulting from the wide range of airspeeds of typical operation (hover to over 100 kn). Also, the rotor degrees of freedom can have a significant impact on the system performance and stability. The importance of the rotor dynamics in the FCS design process is magnified when one realizes that the performance requirements of modern rotorcraft necessitate high-response bandwidth, full-authority FCS. Here, high-response bandwidth refers to the ability of the FCS to produce a desired pilot input/vehicle output response type, e.g., attitude command/attitude hold, over a broad frequency range. While seeking to maximize response bandwidth, the designer is also interested in minimizing feedback bandwidth. As shown in Fig. 1, response bandwidth refers to that associated with y/yc, whereas feedback bandwidth is that associated with y/yf. And, the effects of sensor and actuator dynamics, digital control law implementation, and nonlinear aerodynamic effects further complicate the FCS design process.[1,2]

Traditionally, rotorcraft FCS designers have addressed the described complications by designing an FCS in which a gain scheduler may tune the FCS to the given flight condition with enough gain and phase margin at each flight condition to compensate for unmodeled high-order effects, such as rotor and inflow dynamics. The intent here, however, was to design an FCS utilizing knowledge of the rotor and inflow dynamics that for any flight condition from hover to 100 kn will yield satisfactory performance, obviating a gain scheduling algorithm in the FCS. This work is an extension of that presented in Refs. 3 and 4; the major distinction is that the constrained variable method used in Refs. 3 and 4 was eschewed. To the authors' knowledge, this is the first paper to present quantitative feedback theory (QFT) applied to a 4×4 vehicle model. Considerable effort was directed toward specifying tracking and cross-coupling performance bounds to satisfy handling qualities (HQ) requirements.

Received Feb. 3, 1995; revision received May 10, 1997; accepted for publication June 6, 1997.

*Assistant Professor, Department of Mechanical Engineering. Member AIAA.
†Professor and Vice Chairman, Department of Mechanical and Aeronautical Engineering. Associate Fellow AIAA.

II. QFT

QFT is a technique for designing robust control systems.[3–5] It is a frequency-domain design technique in which uncertainty in the dynamic characteristics of the controlled element is represented as either variation in the coefficients of the control input to response transfer functions or as variation over frequency in the magnitude and phase of the frequency response. Tracking or command-following performance bounds are also considered and are defined as acceptable upper and lower limits of the magnitude on the closed-loop system frequency response.

Consider the multiple-input/single-output (MISO) control system design shown in Fig. 1, where $\mathcal{P} \in P$, P is the set of all possible variations in dynamic characteristics of the controlled element, y is the output, yc is the command, and F and G are the two degrees of freedom (DOF) utilized in the QFT design process. The QFT design methodology utilizes these two design DOF to ensure three design objectives, the first and most important of which is known as stability robustness. Satisfaction of this first design objective is quantified by the following two inequalities:

$$|1 + G\mathcal{P}| > S_1, \qquad \mathcal{P} \in P \tag{1a}$$

$$|G\mathcal{P}/(1 + G\mathcal{P})| > S_2, \qquad \mathcal{P} \in P \tag{1b}$$

where S_1 limits the closest approach of the loop transmission $G\mathcal{P}$ to the $-1 + 0j$ point and S_2 limits the peak magnitude of the closed-loop system. Satisfaction of the second design objective in the QFT process, performance robustness, is quantified by the inequality of Eq. (2), where T_L and T_U represent frequency responses of the upper and lower performance bounds,

$$T_L < FG\mathcal{P}/(1 + G\mathcal{P}) < T_U, \qquad \mathcal{P} \in P \tag{2}$$

Finally, disturbance robustness is desired such that the frequency response due to disturbance inputs remain below some acceptable threshold for any of the possible plant dynamic models. This third design objective is quantified by the inequality

$$\mathcal{P}/(1 + G\mathcal{P}) \leq T_D, \qquad \mathcal{P} \in P \tag{3}$$

Notice that the feedback compensator G, alone, is integral to the satisfaction of Eqs. (1) and (3) and the prefilter F and feedback compensator both are integral to the satisfaction of Eq. (2). A necessary but insufficient condition of Eq. (2), involving only the feedback

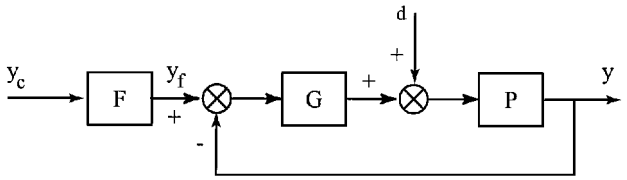

Fig. 1 MISO QFT control problem with disturbance injected before the controlled element.

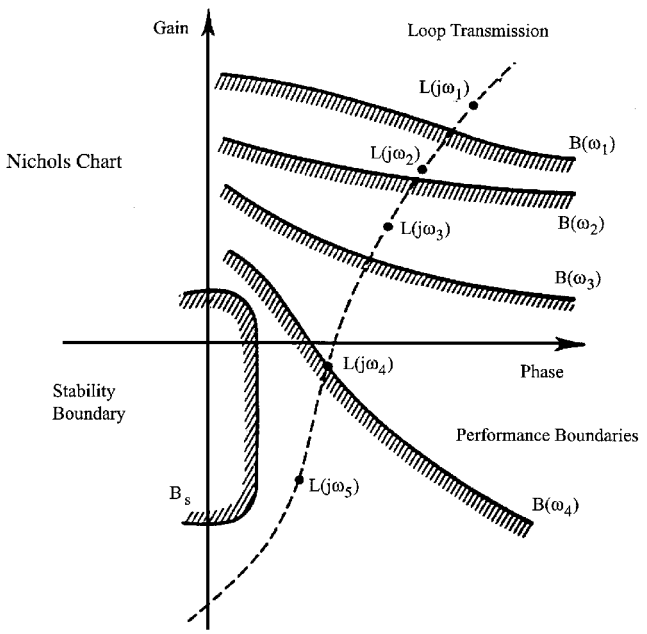

Fig. 2 Design environment for feedback compensation using QFT.

compensator, ensures that the variation in the closed-loop frequency response due to the uncertainty in the dynamic characteristics of the controlled element are within the variations defined across frequency by the performance bounds. This is given by

$$\Delta|G\mathcal{P}/(1+G\mathcal{P})| \leq |T_U| - |T_L| \tag{4}$$

Boundaries $B(\omega_i)$ may be defined on a Nichols chart such that if magnitude and phase of the nominal loop transmission, $L_0(j\omega) = G\mathcal{P}_0(j\omega)$, where $\mathcal{P}_0$ is an arbitrarily selected member of P, at the frequency ω_i are plotted above the boundary, then Eqs. (1), (3), and (4) are satisfied at the frequency. Note that Eq. (1) is satisfied by limiting the approach of the family of loop transmissions, associated with the various members of the set P, to the point (0 dB, 180 deg). This is achieved by forcing the nominal loop transmission to stay below the stability boundary, labeled B_s in Fig. 2. Equation (4) is satisfied at a given frequency by ensuring that the variation in the closed-loop magnitude, resulting from the variation in the set P, is less than the difference between the magnitude of the upper performance bound and the lower performance bound at that frequency. Recognizing that the distance between M-circles, which represent closed-loop magnitude, increases toward the upper right corner of the Nichols chart, it is possible to define a boundary such that, for a given frequency, the inequality of Eq. (4) is satisfied so long as the nominal loop transmission evaluated at that frequency plots above that boundary. Equation (3) is satisfied by requiring a minimum magnitude for the loop transmission at various frequencies and, thus, may be more or less restrictive than the lines defined to satisfy Eq. (4).

Although it is desired that the inequalities specified by Eqs. (1), (3), and (4) be satisfied for all frequencies, this would require an infinite set of specified boundaries and, thus, is not practical. Instead, using the QFT approach, the designer attempts to satisfy these inequalities for a finite set of frequencies spanning a reasonable range. Thus, as shown in Fig. 2, the feedback compensator G is designed such that the nominal loop transmission satisfies the imposed boundaries at each design frequency. The QFT design process is concluded with the determination of the precompensator F in satisfaction with the inequality of Eq. (2). That is, the precompensator F ensures that the closed-loop frequency response $y/y_c(j\omega)$ actually lies between the upper and lower performance bounds T_U and T_L, respectively, given the uncertainty in the controlled element.

To apply QFT to a multiple-input/multiple-output (MIMO) system, a set of MISO systems, mathematically equivalent to the MIMO system and to which the QFT approach is applied independently, must be determined.[6–8] A brief derivation of such a set of MISO systems, based on Schauder's fixed point theorem, follows. In the case of an $n \times n$ MIMO design problem, the input and output vectors $\boldsymbol{y}$ and $\boldsymbol{u}$ are of length n, and $\mathcal{P} \in \boldsymbol{P}$, $\boldsymbol{G}$, and $\boldsymbol{F}$ are square matrices of transfer functions with dimensions $n \times n$. A transform is selected by considering the vector equation defining the closed-loop system,

$$\boldsymbol{y} = \mathcal{P}\boldsymbol{G}(\boldsymbol{F}\boldsymbol{u} - \boldsymbol{y}) \tag{5}$$

so that

$$(\mathcal{P}^{-1} + \boldsymbol{G})\boldsymbol{y} = \boldsymbol{G}\boldsymbol{F}\boldsymbol{u} \tag{6}$$

which yields the constraint that $\mathcal{P}$ must be nonsingular for all of $\boldsymbol{P}$. Now, substituting $\boldsymbol{T}\boldsymbol{u}$ for $\boldsymbol{y}$ in Eq. (6), where $\boldsymbol{T}$ is the matrix of closed-loop transfer functions, we see that

$$(\mathcal{P}^{-1} + \boldsymbol{G})\,\boldsymbol{T} = \boldsymbol{G}\boldsymbol{F} \tag{7}$$

Let each of the elements of the $\boldsymbol{P}^{-1}$ matrix be denoted $1/Q_{ij}$, and require $\boldsymbol{G}$ to be diagonal. To solve this matrix equation, each of the elements of the left- and right-hand sides of the equation must be equated. With a little manipulation of these n^2 equations, a general expression results:

$$T_{ij} = \frac{F_{ij}G_iQ_{ii} + d_{ij}Q_{ii}}{1 + G_iQ_{ii}} \tag{8}$$

where

$$d_{ij} = -\sum_{\alpha \neq i} \frac{T_{\alpha j}}{Q_{i\alpha}} \tag{8a}$$

If the system inputs are assumed to be unit impulse functions, then y_{ij} is equal to T_{ij} and may be substituted for the left-hand side of Eq. (8). In that case, the form of Eqs. (8) and (8a) may be shown graphically by the MISO design problem shown in Fig. 1, allowing the MISO QFT techniques to be utilized in the determination of G_i and F_{ii}. The $T_{\alpha j}$ in Eq. (8a) represent the closed-loop response of the αth output to an impulse in the jth input. Until the system design is complete, these responses are unknown. During the design phase, therefore, these responses are replaced by the acceptable response boundaries τ_{ij}, which represent the largest magnitude for the response assuming the ultimate design satisfies the design constraints. This substitution represents, therefore, a worst-case assumption. Note that for diagonal $\boldsymbol{G}$ compensation, as is assumed here, there exists the additional stipulation that the $\boldsymbol{G}_i$ must satisfy the design constraints for y_{ij} with $j = 1, 4$.

III. UH-60A Blackhawk Helicopter Model

The complexity of the mathematical model to be used in the FCS design is of singular importance. Low-order rigid body models of rotorcraft are satisfactory for the design of low-response bandwidth FCSs, but the limitations on the validity of such models at higher frequencies compromise their utility for the design of high-response bandwidth systems. Utilized in this investigation was a general nonlinear 28th-order rotorcraft model[9] tailored to represent the UH-60A Black Hawk rotorcraft. The model was linearized about six flight conditions ranging from hover to 100 kn at 20-kn increments. Thus, these linearized models defined the possible range for the dynamic characteristics of the rotorcraft and were utilized in the QFT FCS design process. The model included the flapping and lead-lag dynamics of the rotor and the dynamics of the rotor inflow. One addition to the model of Ref. 9 was an actuator for each of the four controls. Each actuator was modeled as a second-order system with a natural frequency of 30 rad/s and a damping ratio of 0.7 (Ref. 10).

IV. MIMO Application of QFT to the UH-60A FCS

Two requisite elements of the MIMO QFT design methodology are the quantification of the variation in possible plant dynamic response and the quantification of acceptable bounds on command tracking and disturbance rejection performance. The first, as was discussed in Sec. III, was provided by the six linearized models of the UH-60A, which constituted the set of possible plant dynamic models $\mathcal{P}$. The other necessary design specification for QFT is the set of boundaries on acceptable performance. It was desired that the defined performance bounds relate to the HQ of the resulting FCS. HQ are defined in Ref. 11 as "those qualities or characteristics of an aircraft that govern the ease and precision with which a pilot is able to perform the tasks required in support of an aircraft role." A rating scale has been developed to standardize pilot evaluation of HQ, which is known as the Cooper–Harper Pilot Opinion Ratings Scale.[12]

Using the military HQ specification,[13] tracking performance boundaries were determined as described in Ref. 14. Unfortunately, the HQ specifications for the cross-coupling responses are written for the demonstration of compliance and are ambiguous when used in design. To determine bounds on cross-coupling performance, therefore, a classical base-line FCS was designed about the 40-kn linear model. The cross-coupling responses of this FCS were evaluated against the HQ specifications, and where acceptable, these responses became the basis for limits on cross-coupling performance. Where peak responses were above acceptable limits, the responses were scaled sufficiently to yield acceptable performance. The resulting performance boundaries utilized in the design process are shown in Tables 1 and 2. Note that, in all of the tables,

$$(\omega) \Rightarrow [(s/\omega) + 1] \qquad [\zeta;\omega] \Rightarrow [(s/\omega)^2 + (2\zeta s/\omega) + 1]$$

To satisfy the design equation (8), it must be true that for $j = 1, n$,

$$\frac{|1 + G_i Q_{ii}|}{|Q_{ii}|} \geq \frac{|d_{ij}|}{|\tau_{ij}|} \tag{9}$$

where τ_{ij} represents the maximum acceptable response of the ith output to the jth input, and

$$|d_{ij}| = \sum_{\alpha \neq i} \frac{|\tau_{\alpha j}|}{|Q_{i\alpha}|} \tag{10}$$

To develop a four-input/four-output FCS (Fig. 3), 16 MISO design problems were addressed for the UH-60 rotorcraft that would yield satisfactory HQ over the range of flight conditions from hover to 100 kn. It was not possible to satisfy all of the design specifications for all 16 of the design problems. Because violation of design specifications in any of the MISO design problems invalidates the mapping of Eq. (9), it was left to discover the true ramifications of these deviations until the final simulation of the FCS with the full rotorcraft model. The resulting feedback compensators and prefilters are listed in Table 3 with the same nomenclature as used in the preceding tables. Note that the maximum order of any of the compensators is only seven. Recalling that the model was of 36th order (28th-order vehicle plus 2nd-order actuators), the compensator simplicity afforded by the frequency-based QFT design is quite apparent. Large-order compensators are frequent results of many modern FCS design techniques, e.g., Ref. 15.

The tracking performance of all four response outputs was satisfactory based on the imposed performance criteria. In addition, by applying the cross-coupling performance criteria from the HQ specification, the cross-coupling responses were also satisfactory. This is despite the fact that the design process indicated that the cross-coupling performance bounds would be violated. Several reasons exist for this apparent inconsistency. First, the cross-coupling performance boundaries were overly restrictive. It may be possible to violate the imposed boundaries and still have satisfactory cross-coupling performance as specified in Ref. 14. Second, as was hinted at earlier, the performance criteria as stated in the specification do not translate directly into frequency-domain bounds. As a result,

Table 1 On-axis performance boundaries

Roll axis	$T_L = \dfrac{0.9}{(3.5)[0.7;\,4.5](10)}$
	$T_U = \dfrac{1.11(5)}{[0.4;\,3.5](10)}$
Pitch axis	$T_L = \dfrac{0.9}{(2.0)[0.7;\,2.6](6)}$
	$T_U = \dfrac{1.11(2.9)}{[0.4;\,2.0](6)}$
Heave axis	$T_L = \dfrac{0.9}{(0.25)(1.0)}$
	$T_U = \dfrac{1.11}{(1.0)}$
Yaw axis	$T_L = \dfrac{0.9}{(3.5)[0.7;\,4.5](10)}$
	$T_U = \dfrac{1.11(5)}{[0.4;\,3.5](10)}$

Table 2 Cross-coupling performance boundaries

	Roll	Pitch	Heave	Yaw
ϕ_c	——	$T_D = \dfrac{1.1(0)}{(0.3)(10)}$	$T_D = \dfrac{0.4(0)}{(0.8)(15)}$	$T_D = \dfrac{20.46(0)}{(0.2)(8)}$
θ_c	$T_D = \dfrac{1.42(0)}{(0.8)(6)}$	——	$T_D = \dfrac{0.71(0)(4)^2}{[0.7;\,1.25][0.3;\,12]}$	$T_D = \dfrac{33.95(0)}{(0.1)(20)}$
$\dot{h}_c$	$T_D = \dfrac{1.83(0)}{(0.6)(6)}$	$T_D = \dfrac{1.68(0)}{(0.3)(5)}$	——	$T_D = \dfrac{-0.06(0)}{[0.2;\,8.5]}$
$\dot{\psi}_c$	$T_D = \dfrac{1.83(0)}{(0.6)(6)}$	$T_D = \dfrac{1.05(0)}{(1)(10)}$	$T_D = \dfrac{0.39(0)}{(0.6)(8)}$	——

Table 3 Prefilters and feedback compensators of the FCS design 1

Roll attitude	$G_\phi = \dfrac{0.0257(0.5)(7.4)[0.7;\,13.72][0.7;\,30]}{(0)(20)[0.7;\,40][0.7;\,50](67.2)}$	$F_{\phi\phi_c} = \dfrac{(0.64)(2)}{(0.5)(7)[0.7;\,10]}$
Pitch attitude	$G_\theta = \dfrac{0.0185(0.15)(0.7)(1)(1.6)[0.7;\,30]}{(0)^2(6)(80)^2[0.7;\,80]}$	$F_{\theta\theta_c} = \dfrac{1}{[0.7;\,2.52]}$
Vertical velocity	$G_{\dot{h}} = \dfrac{0.306(0.5)}{(0)(60)}$	$F_{\dot{h}\dot{h}_c} = 1.0$
Yaw rate	$G_{\dot{\psi}} = \dfrac{0.4192(2)[0.7;\,30]}{(0)(42)[0.7;\,50](70)}$	$F_{\dot{\psi}\dot{\psi}_c} = \dfrac{1}{[0.7;\,4.2]}$

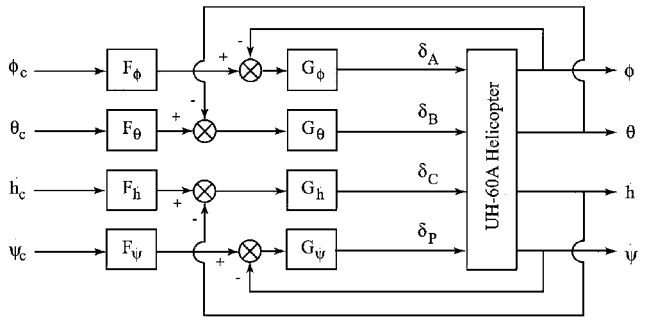

Fig. 3 FCS schematic block diagram.

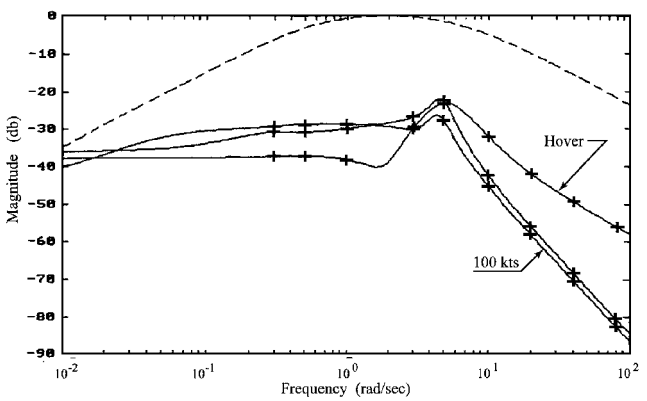

Fig. 4 Approximate frequency response of roll attitude due to yaw rate command, design 1.

many different boundaries could be drawn in the frequency domain, each of which would satisfy the performance criteria set forth in the HQ specification. Third, disturbance magnitudes for the equivalent MISO design problems are overspecified, as explained earlier. Therefore, it was unclear whether actual performance bounds were violated or whether, instead, the conservative worst-case estimate of the various vehicle response modes caused the boundary violations but the actual closed-loop responses were compliant with the specified bounds.

To investigate this further, an abbreviated form of the Golubev algorithm,[16] which computes a rational function approximation, $H(s) = \text{num}(s)/\text{den}(s)$, given input and output time series, was employed. Figure 4 presents a plot of the approximate closed-loop frequency response of roll attitude due to yaw rate command for three flight conditions: hover, 40 kn, and 100 kn. Also included on the plot as a dashed line is the cross-coupling performance bound. Clearly, all three frequency responses are well below the imposed boundary at each of the design frequencies indicated by + marks in Fig. 4. This is contrary to the design procedure, which indicated that this cross-coupling performance bound would be violated by the FCS design. This inconsistency must in large part be due to the overly conservative nature of the determination of the disturbance magnitude for the MISO design problems.

If the assumption of a diagonal G feedback compensator matrix is foregone, additional flexibility is gained,[17] as Eq. (8a) becomes

$$d_{ij} = \sum_{\alpha \neq i} T_{\alpha j}\left(G_{i\alpha} - \frac{1}{Q_{i\alpha}}\right) \tag{11}$$

The off-diagonal elements of the $\boldsymbol{G}$ feedback compensator matrix can be used to reduce the magnitude of the cross-coupling responses if these elements of $\boldsymbol{G}$ are determined so as to minimize the magnitude

$$|G_{ij} - (1/Q_{ij})| \tag{12}$$

Unfortunately, the magnitude of Q_{ij} tends to diminish at higher frequencies. Thus, to satisfy Eq. (12), the magnitude of G_{ij} must increase at higher frequencies, which results in an undesirable increase in the system's sensitivity to noise.

V. Sequential Loop Closure

One problem arising from the conservative determination of the disturbance signals for the MISO design problems is that the resulting feedback compensator designs are overly conservative. A price paid for using the aforementioned design technique is that the resulting control system has increased sensitivity to noise. This is termed by Horowitz[3] the cost of feedback and is characterized by large Bode magnitudes in the feedback compensator at high frequency. The conservative nature of this design technique is clearly evident in the design described in Sec. IV. Also, although many performance bounds were unavoidably violated in the design process, adequate cross-coupling performance was nonetheless attained. Although the fact that adequate cross-coupling performance was attained speaks well for the design methodology that was utilized in the creation of the FCS, it is unfortunate that this performance was not foreseen during the design process.

The QFT control system design methodology for the MIMO design problem is founded on the assumption that all of the bounds for all of the n^2 design problems are being met by the compensators. Without this, the mathematical foundation for the technique is violated, and the proof of the equivalence between the n^2 MISO design problems and the original MIMO design problem no longer applies. A better design approach is necessary for the design of a robust MIMO FCS for the UH-60 rotorcraft.

One improvement to the extension of the MISO QFT technique to the MIMO control system design problem is offered in Ref. 7. This method, termed sequential loop closure (SLC), utilizes available closed-loop response information to reduce the overspecification of the disturbance signal in the design of successive feedback compensators. Note from Eq. (8) that the closed-loop response of all output variables to a given input is required to define the disturbance signal of the MISO equivalent system. This information is, of course, unavailable prior to the FCS design, and so the worst-case upper performance boundaries were used in the design method of Sec. IV. After one set of MISO systems has been analyzed, resulting in the design of a G_i and a set of F_{ij} for $j = 1, 4$, then the closed-loop system response of the ith output to all inputs is fully defined. Thus, this information may be used in the definition of the disturbance signal for subsequent analysis in place of the worst-case assumption, reducing the overspecification in those designs. Ideally, once three of the four sets of MISO systems have been analyzed, the disturbance signal for the fourth set can be specified exactly, eliminating all overspecification in the design of the last feedback compensator. The algebra entailed in applying this concept is rather daunting and is presented in Ref. 18.

The order of loop closure is arbitrary, and there is no guidance to aid the designer in selecting an order. Intuitively, it is obvious that as the overspecification of the disturbance signal decreases, it becomes easier to satisfy the imposed disturbance rejection boundaries. Thus, if one is encountering difficulties in satisfying the disturbance rejection boundaries for a particular loop when using the design procedure described in Sec. IV, that loop should be closed later rather than earlier in the sequential process. Beyond this, however, there is no apparent way to choose the sequence. Two different sequences for loop closure were attempted in this study. For the sequence in which the roll loop was the final loop closed, all performance boundaries were satisfied in the FCS design. The feedback compensators and prefilters for this design are listed in Table 4.

Once again, the FCS resulting from this design technique produced satisfactory results for all responses. Figure 5 shows the approximate closed-loop frequency response of roll attitude due to yaw rate command for three flight conditions: hover, 40 kn, and 100 kn for this FCS. A comparison with Fig. 4 demonstrates a significant degradation in performance for the SLC FCS in that the cross-coupling response has a greater magnitude in Fig. 5. This degraded response is still adequate, however, as defined by the dashed cross-coupling performance boundary. The implication is that, while still attaining acceptable performance, the SLC FCS is less conservative than the FCS described in Sec. IV, hereafter referred to as

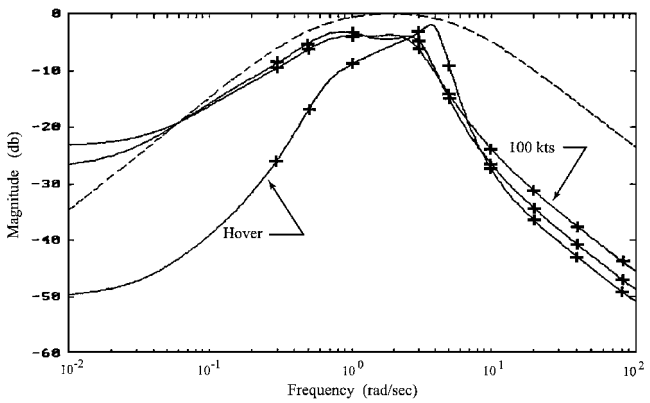

Fig. 5 Approximate frequency response of roll attitude due to yaw rate command, SLC design.

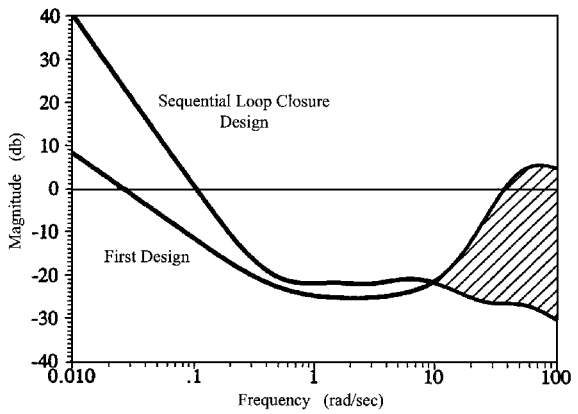

Fig. 6 Comparison of feedback compensators for the roll axis, G_ϕ design 1 and SLC design.

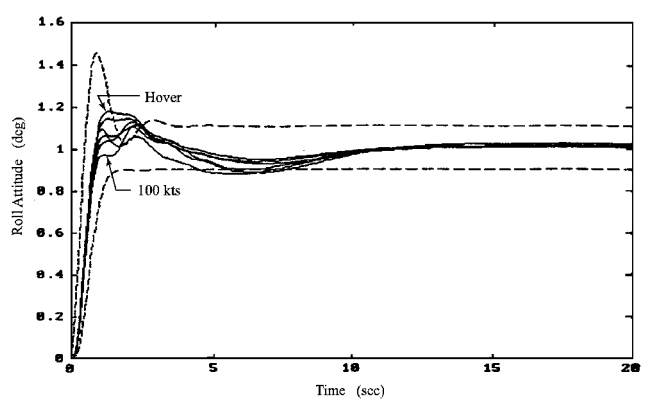

Fig. 7 Roll attitude response to a unit step in roll attitude command.

design 1. This is shown graphically in Fig. 6, a comparison of the roll loop feedback compensators G_2, for design 1 and the SLC design. The shaded area represents the reduced cost of the improved roll attitude compensator.

The on-axis responses, e.g., roll attitude response to a unit step change in roll attitude command, etc., for the SLC design are shown in Figs. 7–10. The dashed lines represent the upper and lower tracking performance boundaries. Each solid line represents the response of the rotorcraft at a different flight condition, ranging from hover to 100 kn. Note that the apparent violation of the imposed tracking performance boundaries are due to the translation of the frequency-domain boundaries into the time domain. The performance boundaries, defined in the frequency domain, indicate limits on rise time, settling time, overshoot, and steady-state error. They do not represent limits on the output at specific instances in time. Off-axis responses for pitch attitude response to a unit step change in roll attitude command and to a unit step change in vertical velocity command are shown in Figs. 11 and 12. Although the performance

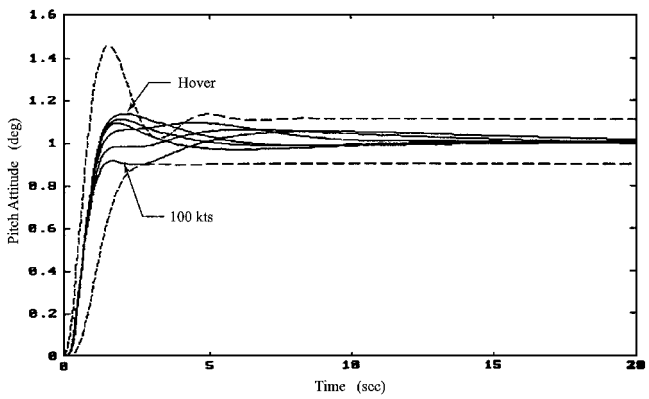

Fig. 8 Pitch attitude response to a unit step in pitch attitude command.

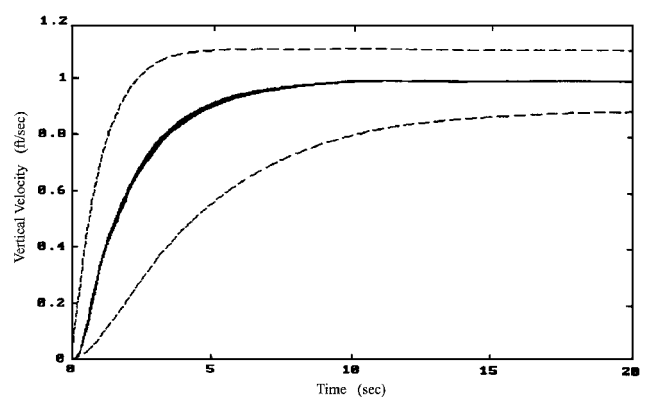

Fig. 9 Vertical velocity response to a unit step in vertical velocity command.

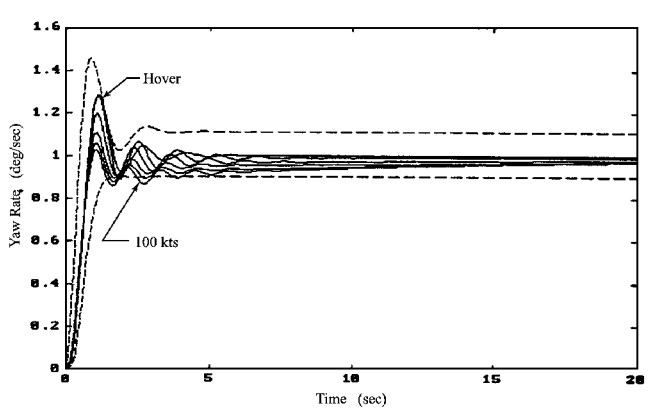

Fig. 10 Yaw rate response to a unit step in yaw rate command.

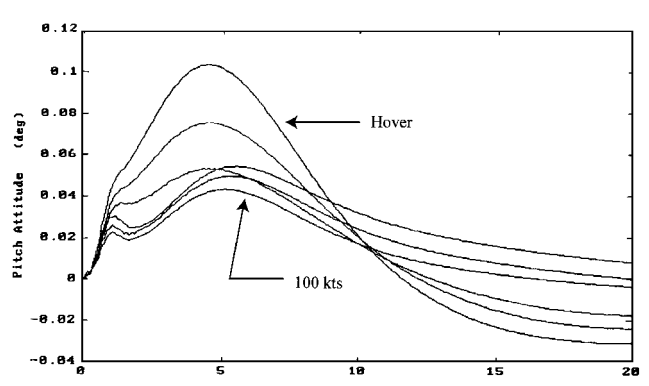

Fig. 11 Pitch attitude response to a unit step in roll attitude command.

Table 4 Prefilters and feedback compensators of the FCS SLC design

Roll attitude	$G_\phi = \dfrac{0.0257(0.5)[0.9;\ 0.5](2.76)[0.7;\ 3][0.7;\ 30]}{(0)^2(2)^2(2.5)(6)^2[0.7;\ 50]}$	$F_{\phi\phi_c} = \dfrac{(0.25)(0.88)(1)}{(0.3)(0.36)(4.64)}$
Pitch attitude	$G_\theta = \dfrac{0.0185(0.15)(0.7)(1)(1.6)(10)[0.7;\ 30]}{(0)^2(6)(80)^2[0.7;\ 80]}$	$F_{\theta\theta_c} = \dfrac{1}{[0.7;\ 2.76]}$
Vertical velocity	$G_{\dot h} = \dfrac{0.306(1)(32)}{(0)(8)}$	$F_{\dot h\dot h_c} = \dfrac{(10)}{(0.5)(5)}$
Yaw rate	$G_{\dot\psi} = \dfrac{0.4192(5.2)[0.7;\ 30]}{(0)[0.7;\ 50](70)}$	$F_{\dot\psi\dot\psi_c} = \dfrac{(2)}{[0.7;\ 2.5]}$

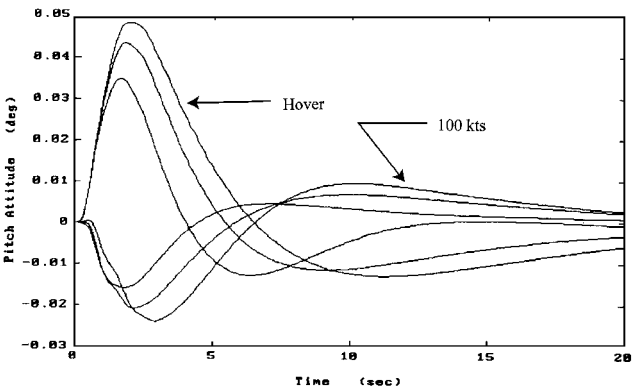

Fig. 12 Pitch attitude response to a unit step in vertical velocity command.

boundaries do not lend themselves to depiction in the time domain, these responses are well within the level 1 HQ limits as represented in Ref. 13.

VI. Conclusions

The extension of the MISO QFT design technique to a MIMO design problem results in an overly conservative control system design. It may not even be possible to satisfy all of the QFT design criteria due to the overspecification of the performance bounds associated with this technique. This problem is more acute with greater numbers of inputs and outputs. To address this problem in the 4×4 MIMO FCS design for the UH-60A, a technique known as SLC was utilized. With this technique, the overspecification of the performance boundaries is reduced with each successive loop closure, allowing for a less conservative FCS design. Another possible means of alleviating the overdesign issue in the MIMO design technique would be to address the cross-coupling characteristics of the MIMO system directly because it is the cross-coupling characteristics of the MIMO system that result in the overspecification of the performance boundaries in the extension of the MISO design technique. This could be accomplished by implementing off-diagonal elements to the feedback compensator matrix, as described in Sec. IV.

Overall, QFT does provide a good means of designing a robust rotorcraft FCS, particularly when SLC is utilized. The FCS designed utilizing this technique demonstrated acceptable dynamic responses for a wide range of flight conditions using a realistic vehicle model.

Acknowledgments

This research was supported by NASA Grant NCC2-624, NASA Ames Research Center, Moffett Field, California. The grant Technical Manager was Mark B. Tischler of the Aeroflightdynamics Directorate, whose assistance and advice were greatly appreciated.

References

[1]Tischler, M. B., "Digital Control of Highly Augmented Combat Rotorcraft," NASA TM-88344, May 1987.

[2]Chen, R. T. N., and Hindson, W. S., "Influence of High-Order Dynamics on Helicopter Flight-Control System Bandwidth," *Journal of Guidance, Control, and Dynamics*, Vol. 9, No. 2, 1986, pp. 190–197.

[3]Horowitz, I., "Quantitative Feedback Theory (QFT)," *Proceedings of the 1988 American Control Conference*, Vol. 3, 1988, pp. 2032–2037.

[4]Horowitz, I. M., and Sidi, M., "Synthesis of Feedback Systems with Large Plant Ignorance for Prescribed Time-Domain Tolerances," *International Journal of Control*, Vol. 53, No. 2, 1972, pp. 287–309.

[5]Horowitz, I., "Survey of Quantitative Feedback Theory (QFT)," *International Journal of Control*, Vol. 53, No. 2, 1972, pp. 255–291.

[6]Horowitz, I., and Loecher, C., "Design of a 3×3 Multivariable Feedback System with Large Plant Uncertainty," *International Journal of Control*, Vol. 33, No. 4, 1981, pp. 677–699.

[7]Horowitz, I., "Improved Design Techniques for Uncertain Multi-Input-Multi-Output Feedback Systems," *International Journal of Control*, Vol. 36, No. 6, 1982, pp. 977–988.

[8]Horowitz, I., Yaniv, O., Golubev, B., and Neumann, L., "A Synthesis Technique for Highly Uncertain and Interacting Multivariable Flight Control Systems," *IEEE Transactions*, 1981.

[9]Takahashi, M. D., "A Flight-Dynamic Helicopter Mathematical Model with a Single Flap-Lag-Torsion Main Rotor," NASA TM 102267, Feb. 1990.

[10]Howlett, J. J., "UH-60A Blackhawk Engineering Simulation Program, Vol. 1—Math Model," NASA CR-166309, Dec. 1981.

[11]Harper, R. P., and Cooper, G. E., "Handling Qualities and Pilot Evaluation," *Journal of Guidance, Control, and Dynamics*, Vol. 9, No. 5, 1986, pp. 515–529.

[12]Cooper, G. E., and Harper, R. P., "The Use of Pilot Rating in the Evaluation of Aircraft Handling Qualities," NASA TN D-5153, April 1969.

[13]MIL-SPEC, "Handling Qualities Requirements for Military Rotorcraft," U.S. Army Aviation Systems Command, ADS-33C, Aug. 1989.

[14]Hess, R. A., and Gorder, P. J., "Quantitative Feedback Theory Applied to the Design of a Rotorcraft Flight Control System," *Journal of Guidance, Control, and Dynamics*, Vol. 16, No. 4, 1993, pp. 748–753.

[15]Takahashi, M. D., "Helicopter Flight-Control Design Using an H2 Method," *Proceedings of the AIAA Guidance, Navigation, and Control Conference*, Vol. 3, AIAA, Washington, DC, 1991, pp. 1392–1416.

[16]Golubev, B., and Horowitz, I., "Plant Rational Transfer Function Approximation from Input-Output Data," *International Journal of Control*, Vol. 36, No. 6, 1982, pp. 711–723.

[17]Catapang, D. R., Tischler, M. B., and Biezad, D. J., "Robust Crossfeed Design for Hovering Rotorcraft," Symposium and Tutorial on Quantitative Feedback Theory, Dayton, OH, Aug. 1992.

[18]Gorder, P. J., "A Robust Flight Control System Design Methodology Utilizing Quantitative Feedback Theory (QFT)," Ph.D. Dissertation, Dept. of Mechanical and Aeronautical Engineering, Univ. of California, Davis, CA, July 1993.